Journal of Clinical Monitoring and Computing (2008) 22:11–22
DOI: 10.1007/s10877-007-9102-z

DESCENDING AORTIC FLOW CONTRIBUTION TO INTRATHORACIC IMPEDANCE—DEVELOPMENT AND PRELIMINARY TESTING OF A DUAL IMPEDANCE MODEL

A. Barry Baker, MBBS, DPhil, FANZCA, FJFICM, FRCA[1,4], Chris N. McLeod, MA, MSc, DPhil, MIPEM[2], Alastair J. Roxburgh, MSc, MIEEE[1] and Paul Bannister, BSc (Hons), PhD[3]

Baker AB, McLeod CN, Roxburgh AJ, Bannister P. Descending aortic flow contribution to intrathoracic impedance—development and preliminary testing of a dual impedance model.
J Clin Monit Comput 2008; 22:11–22

ABSTRACT. Objective. Impedance measurement of cardiac output has struggled to become established partly because there have been only a few attempts to establish a sound theoretical basis for this measurement. Our objective is to demonstrate that there is valuable aortic flow information available from an intrathoracic impedance signal which may eventually be useful in the measurement of cardiac output by impedance technology. **Methods.** A model, using dual impedance measurement electrodes and the change in impedance when blood flows, has been developed based on an intrathoracic impedance model of the descending aorta and esophagus. Using this model as the basis for measurement by an esophageal probe, we provide solutions to the velocity of blood flow in the descending aorta. **Results.** Five patients were studied. Only three patients had suitable signals for analysis but the aortic flow profiles from these three patients were consistent and realistic. **Conclusion.** Aortic blood flow information may be obtained from the intrathoracic impedance signal using this dual impedance method.

KEY WORDS. itrathoracic impedance, aortic flow, model.

INTRODUCTION

For over 60 years there has been fluctuating interest in electrical impedance measurements of various regions of the body [1–17]. This interest followed earlier electrical experiments by a number of workers who used similar methods [18–20]. Thoracic impedance has had considerable research energy expended on its elucidation and validation, and has reached such respectability that NASA has used it to monitor astronauts' cardiac function and lung water, and some intensive care units use the technique for the measurement of cardiac output in critically ill patients, though there have been conflicting reports of its validity [21–30]. If a reliable and valid impedance measurement of cardiac output were able to be developed it would be most useful, as the current standard method using pulmonary artery catheterisation and thermodilution has reliability and methodological problems as well as reportedly causing increased morbidity and mortality [31–33].

In the last twenty years an esophageal probe approach has been used to attempt to improve the derived impedance signal by improving signal to noise ratio [34–37]. Mitchell and Newbower [34] have, however, argued that this technique is unlikely to yield satisfactory results because

From the [1]Department of Anaesthesia and Intensive Care, University of Otago, Dunedin, New Zealand; [2]School of Technology, Oxford Brookes University, Oxford, UK; [3]Department of Mathematics, University of Otago, Dunedin, New Zealand; [4]University of Sydney, Sydney, NSW 2006, Australia.

Received 20 May 2007. Accepted for publication 22 October 2007.

Address correspondence to A. B. Baker, University of Sydney, Sydney, NSW 2006, Australia.
E-mail: bbaker@usyd.edu.au

"the major determinant of the impedance signal associated with ejection will be aortic motion, and not aortic distension"—that is, there is an inability to distinguish total aortic movement from blood flow. This conclusion was based on the analysis of a biomathematical model devised by them. Our present work extends the theory derived from the same model, which claims to measure aortic blood flow from an esophageal probe, with two major developments: firstly, inclusion of the impedance change occurring due to the flow of blood in the aorta (which was neglected by Mitchell and Newbower in their analysis), and secondly, the use of two simultaneous impedance measurements which allows a solution which is independent of the component due to lateral aortic displacement, the most significant unknown variable. Our aim is to demonstrate that there is aortic flow information available from the esophageal intrathoracic impedance signal.

MATHEMATICAL MODEL AND SOLUTION

The anatomical model used is shown in Figure 1. This model is similar to that used by Mitchell and Newbower [34], with the additions of an electrical conductivity change which occurs when blood flows and of a second pair of voltage sensing electrodes. The model is anatomically valid for the esophageal intrathoracic impedance method if the electrodes are situated close to and parallel to the descending aorta where it lies adjacent to the esophagus in the lower thorax, but is not valid for positions which are higher in the chest, nor if electrodes stray into the stomach. The Mitchell and Newbower model, which has the same anatomical validity, did not take account of the increase in the electrical conductivity of blood which occurs when blood flows [38–41]. Because this fractional change in electrical conductivity of blood may be 10–25% for peak flows, there is an error in their findings.

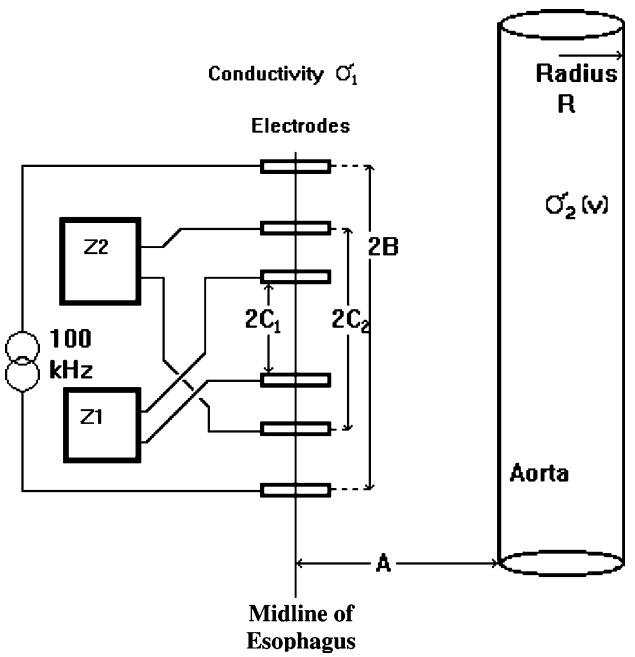

Fig. 1. Simplified model of the dual impedance method. Z = impedance measurement; 100 kHz = current source; σ_1 = thoracic electrical conductivity; $\sigma_2(v)$ = electrical conductivity of blood as a function of velocity; 2B, $2C_1$ and $2C_2$ = electrode spacing distances; A = distance between esophageal probe and aorta.

In the simplified anatomical model (Figure 1) the aorta is represented as an infinite rigid cylinder of conductivity σ_2(v) (a function of blood velocity v) and radius R, passing through the thorax represented as an infinite homogeneous medium with electrical conductivity σ_1. A four-electrode esophageal probe is aligned parallel to the lumen of the aorta at a distance **A** from it. **B** and $\mathbf{C_1}$ & $\mathbf{C_2}$ are respectively the half-spacings of the current source and voltage sensing electrodes of the probe. There may be more than two pairs of voltage sensing electrodes used if further mathematical analysis were to be carried out. This model is similar to that used by Mitchell and Newbower [34], with the addition of σ_2, the electrical conductivity of blood now defined to be a function of velocity, and with the addition of another pair of sensing electrodes. Mitchell and Newbower derived their solution to Maxwell's equations using a conformal transformation and the method of images. Thus the solution, incorporating the change in conductivity with change in blood velocity, becomes:

$$Z_i(v) = \frac{1}{2\pi\sigma_1}\left[2\frac{C_i}{B^2 - C_i^2} + \frac{\sigma_2(v) - \sigma_1}{\sigma_2(v) + \sigma_1} I_i\right] \tag{1}$$

where

$$I_i = \frac{1}{\sqrt{X^2 + (B + C_i)^2}} - \frac{1}{\sqrt{X^2 + (B - C_i)^2}}, \quad i = 1, 2 \tag{1a}$$

and

$$X = 2A + \frac{A^2}{R} \tag{1b}$$

The electrical conductivity of blood increases by at least 10% for peak flows, and the approximate relationship (adapted from Visser et al. [39, 40]) is,

$$\Delta\sigma_2 = \sigma_2(0)a[1 - e^{-b\sqrt{v}}] \tag{2}$$

where $\sigma_2(0)$ refers to the electrical conductivity of blood during the diastolic (no flow) phase. Reversed flow

conditions are not addressed in the model, because impedance changes due to flow are not directional.

For a hematocrit of 45%, and a 12% change in σ_2 with change in aortic flow:

$$\mathbf{a} \approx -0.17$$

$$\mathbf{b} \approx 0.15\,(\mathrm{cm/s})^{-1/2}$$

In the case where only one pair of voltage sensing electrodes is used, and differentiating Equation (1) with respect to σ_2, and substituting for $\Delta\sigma_2$ as given by Equation (2), we get an equation relating the measured change in impedance (ΔZ) value to the velocity of blood in the aorta,

$$\Delta Z(v) = \frac{-\sigma_2(0)aI(1 - \mathrm{e}^{-b\sqrt{v}})}{\pi(\sigma_1 + \sigma_2(0))^2} \tag{3}$$

Rearranging Equation (3), and changing from v to t as the independent variable, the instantaneous velocity of blood flowing in the aorta may be calculated as a function of $\Delta Z(t)$,

$$v(t) = \left[\frac{1}{b}\ln\left(1 + \frac{\Delta Z(t)\pi(\sigma_1 + \sigma_2(0))^2}{\sigma_2(0)aI}\right)\right] \tag{4}$$

This expression describing the electrical impedance measured according to our model, in respect of variable $\boldsymbol{I}$, involves the variables **A**, **B**, **C**, **R** which are distances. **B** and **C** are fixed, as they are distances on the probe. **A** is the unknown distance between the esophagus and the descending aorta, and the expression is very sensitive to its value. **R** is the unknown radius of the descending aorta which may be estimated for the adult population (~1.25 cm), or measured by ultrasound, CT or MRI if further accuracy is desired, though **A** cannot. By making simultaneous measurements of the impedance using one pair of current electrodes (determining **B**) and two pairs of voltage electrodes (determining $\mathbf{C_1}$ and $\mathbf{C_2}$), two impedance traces are obtained ($Z_1(t)$ and $Z_2(t)$). The impedance values from these traces can be digitised and the expressions solved simultaneously to eliminate **X** (which is related to both **A** and **R**) and give an instantaneous value for $\sigma(v)$. From this an instantaneous value for the blood velocity **v** may be derived. An estimate of the stroke volume in this aortic segment may then be calculated.

During much of the cardiac cycle the spatial velocity profile in the descending aorta is approximately constant due to flow shear near the aortic walls [42] and because the blood is accelerating. Thus the aortic blood flow can be approximated by a single vector quantity $\mathbf{v}(\mathbf{t})$ that has a single component $v(t)$ in the downward direction. Stroke volume through the aortic segment can therefore be calculated from the relationship

$$\mathrm{SV} = \pi R^2 \int_{t1}^{t2} v(t)\mathrm{d}t \tag{5}$$

where $t_2 - \mathrm{t}_1$ is the time that the aortic valve is open. Therefore from Equation (4) we have,

$$\mathrm{SV} = \frac{\pi R^2}{b^2}\int_{t_1}^{t_2}\left[\ln\left(1 + \frac{\Delta Z(t)\pi(\sigma_1 + \sigma_2(0))^2}{\sigma_2(0)aI}\right)\right]^2 \mathrm{d}t \tag{6}$$

With the single-channel intrathoracic (esophageal) technique, interpretation of the ΔZ signal is complicated by the strong dependence of baseline thoracic impedance (Z_0) and ΔZ on the distance between the probe and the aorta (**A**). However the maximum $|\Delta Z|$ can be used as described, because there is minimal aortic movement until after peak flow is achieved [43] and the two-channel technique eliminates **A**. If we concern ourselves only with the maximum value of $|\Delta Z(t)|$, and approximate the aortic blood flow as a simple triangle wave from t_1 to t_2, then Equation (6) may be simplified, and stroke volume becomes

$$\mathrm{SV} = \frac{\pi R^2(t_2 - t_1)v(t)_{\max}}{2} \tag{7}$$

where $v(t)_{\max}$ is calculated from $|\Delta Z(t)|_{\max}$, using Equation (3). Stroke volume can thus be obtained from the impedance change occurring with blood flow. The stroke volume in this aortic segment will be only the descending aortic component of the cardiac stroke volume, due to the low thoracic position of measurement in this model. The assumptions on which this model depends are listed in Table 1.

EXPERIMENTAL METHODS

The Otago Hospital Board's Ethics Committee approved the project and informed consent was obtained from the patients and their surgeons. Five patients were studied who were having surgery for coronary artery bypass grafting, and these patients were studied on their return to the intensive care unit where they continued to be ventilated and heavily sedated with diazepam and opiates following the usual clinical practice at that time. A multi-electrode esophageal impedance probe with six electrodes (at 2 cm spacing, so **B** = 5 cm, $\mathbf{C}_2$ = 3 cm, $\mathbf{C}_1$ = 1 cm) was placed after return of each patient to the intensive care unit and measurements were carried out in periods of relative cardiovascular stability. The probe was positioned at all times by visual means with the most proximal electrode just into the esophagus. Chest X-rays were

Table 1. Assumptions inherent in the dual impedance model

Cylindrical aorta parallel to esophagus and which moves uniformly.
Other impedance contributions (e.g. from the heart) are minimised by assuming that the aorta is the most proximal blood organ to the esophagus over the measurement interface.
Blood flow induces impedance changes according to the Visser equations [39, 40] with forward laminar flow along the aorta.
There is minimal rotational contribution in blood flow to the impedance signal.
Dual impedance method allows the elimination of the main unknown variable "A"—the distance between the esophageal probe and the aorta.
Initial changes in $\|\Delta Z\|$ up to the maximum are free of aortic movement, and consist of forward aortic flow only.
Positive and negative velocity are inseparable, therefore velocity equates to speed in this situation because |velocity| = speed.
Aortic radius is assumed (1.25 cm for adults) but could be measured by ultrasound, CT or MRI—this measurement is only needed for aortic stroke volume calculations, and is not required for aortic flow velocity.

routinely taken for clinical care which confirmed the longitudinal position of the probe, and an electrical signal was then established from the most distal electrode. No signal would have been obtained if the probe had been too far into the esophagus with the distal electrode in the stomach. The probe position at the patient's teeth was then kept constant and checked regularly as the impedance traces, and the velocities calculated from them, were very sensitive to even small changes in the esophageal position of the electrodes.

The impedance signal was generated by an impedance analyzer built for this study, but based on a simple analyzer design in use by the University of Otago Physiology Department for limb impedance plethysmography. It used a 4 mA rms 100 kHz constant current source signal with a 1k series resistance, together with an envelope detector and high- and low-pass filters. The resultant ΔZ and Z_0 signals were displayed on a Hewlett Packard 7400 thermal strip chart recorder. Depending on the probe electrode configuration, the peak to peak amplitude of the cardiac-synchronised ΔZ impedance was 2.5 Ω with a range of 0.7–4 Ω, with typical Z_0 signals in the range of 3–16 Ω. The current output was used between the two outer electrodes on the esophageal probe. Estimates of descending aorta blood flow were made from the intrathoracic impedance after suitable computation based on our theoretical model. At least three good traces within 10% of each other were generated in a standard manner with respiratory synchronisation, and at times when the patients were considered to be cardiovascularly stable. Representative impedance traces are shown in Figure 2.

The traces were sampled at 40 ms intervals for complete cardiac cycles. The cycles were always taken at end-expiration. These pairs of values were used to calculate an instantaneous value of $\sigma(\nu)$. The values of **A** were checked to determine that they were positive and of a reasonable magnitude given a normal adult value for **R**. The calculation of blood velocity from the values of $\sigma(\nu)$ depended

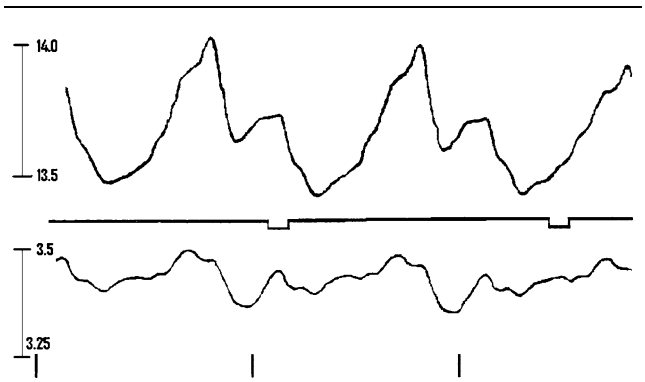

Fig. 2. Representative intrathoracic impedance traces. Top trace delta-Z (ΔZ_2) waveform from sensing electrodes C = 2 cm. Second trace: time marker (s). Third trace delta-Z (ΔZ_1) waveform from sensing electrodes C = 1 cm. Fourth trace ECG marker (R peak).

on the conductivity of the patient's blood when it was at rest. It was assumed that the minimum conductivity found during any cycle corresponded with a blood velocity of zero and that there was no reverse flow, an important consideration because (as stated previously) blood conductivity changes due to flow are independent of the direction of flow. The minimum conductivity value was then used in the calculation of the velocity at the other sample times in that cycle. The minimum conductivities were checked to ensure that they were consistent during a study. Unfortunately, it was not possible to make independent measurements of blood conductivity in vitro to confirm the minimum value.

RESULTS

Figure 3 shows typical traces of ΔZ_1, ΔZ_2 and the derived velocities for patient T at each sample point throughout a cardiac cycle starting with the R wave of the EKG. Each

impedance value is the average over three cardiac cycles, taken in late expiration or end-expiration. The averaging was achieved by aligning the peak of the R-waves of the ECG trace for the three cycles. Typically, the impedance change detected at the wider pair of electrodes was about 0.3 Ω on a base of 14 Ω, and 0.1 Ω on a base of 3 Ω for the closer pair of electrodes.

Only three of the five patients had repeatable impedance signals and the velocity waveforms used were derived from each of these three patients (Table 2). Flow profiles from these three patients were consistent and realistic and are presented in Figure 4. Table 2 and Figures 3 and 4 emphasise the reproducibility of the impedance traces which produced these velocity measurements, despite the original impedance traces often seeming to be markedly different.

DISCUSSION

The velocity profiles shown in Figure 4 are completely consistent with other studies in the descending aorta as demonstrated in McDonald's classic text [42]. As previously reported [36], the signal-to-noise ratio of the cardiac component of the impedance signal is 25 times better by the intrathoracic approach when compared with the transthoracic. This is a major advantage of the intrathoracic probe, though the proximity to the heart and other large blood vessels creates some problems in interpretation which may have been responsible for the poor impedance traces in the results which had to be rejected, and which are likely to be less significant in the transthoracic approach. This is demonstrated by the variability of the inter-patient impedance traces and the sensitivity of the intra-patient traces to very small displacements of the electrodes. As **A** increases the impedance changes and sensitivity decreases, and as seen in Figure 5 (derived by the authors from CT images) the esophageal electrodes may be in close proximity to the heart and aortic arch in certain configurations. We minimised the aortic arch effects by using distal electrodes for our measurements.

Previously accepted methods of calculating stroke volume from thoracic impedance change were those of Kedrov [44], Bonjer [45] and Nijboer [46], which were modified by Patterson [47] and Kubicek [5]. These methods were derived from the assumption of a cylindrical model for a blood vessel in a limb, which was then transposed with little alteration to a model of the thorax [47]. There are greater assumptions necessary for that model than there are for our model, though obviously our model still needs further modification. Nevertheless transthoracic impedance measurement has attained a degree of acceptance as a valid means for measuring cardiac output, and there has been a rapid increase in the number of commercial transthoracic impedance machines designed to measure cardiac output [30, 48].

Using the Patterson/Kubicek equations [47] to calculate cardiac output from intrathoracic impedance gives very high values—approximately 20–30 times too large. This is not surprising since all the current passes through regions of large blood movements, whereas with surface electrodes the majority of the current passes through the subcutaneous, conductive muscle sheets. The very primitive models which have been developed for the transthoracic method have no anatomical specificity. The cardiac-synchronous component of the impedance signal is an unquantifiable amalgamation of signals from each of the following—blood displacement, blood volume and blood flow in all the tissues and vessels of the thorax. Also the requirement to differentiate the impedance signals in these equations magnifies the noise sensitivity associated with the signals by approximately +6 dB/octave rise in the frequency response.

Sramek [49] modified the cylindrical model, changing to a truncated cone and Bernstein [50] has further amended this equation to produce the currently used version. The Kubicek equation has also been further modified by De Mey and Enterling [51] and van der Meer's group [14] who then showed that there was no difference between their modified Kubicek equation and the Bernstein/Sramek equation provided there was correct electrode positioning appropriate for each technique [14]. There have been variable results with the Bernstein/Sramek transthoracic technique [26, 27, 52, 53] though the technique has been used intrathoracically to calibrate cardiac output with very good correlation to thermodilution [37]. Also Imhoff et al. [54] have modified the Tishchenko [55] equation for whole body impedance, but their results were not convincing. Balestra et al. [37] have shown very good comparisons using an esophageal probe and the BoMed NCCOM3-Revision 4 impedance monitor with a distance between electrodes of 25.5 cm. Recently, however, Patterson and his group [56] have been very pessimistic about the method when investigating an animal model with an electromagnetic flow transducer on the ascending aorta.

There are sound theoretical reasons why the transthoracic impedance approach is likely to have major errors [57, 58]. The development of an anatomically specific model by Mitchell and Newbower [34], however, offers a starting point for a scientific description of a very complex situation. Theoretically our solutions have shown that at least as much measured impedance change is due to change in blood flow speed in the aorta as is due to aortic displacement, which is mathematically removed in the dual impedance model [41], and represents the major

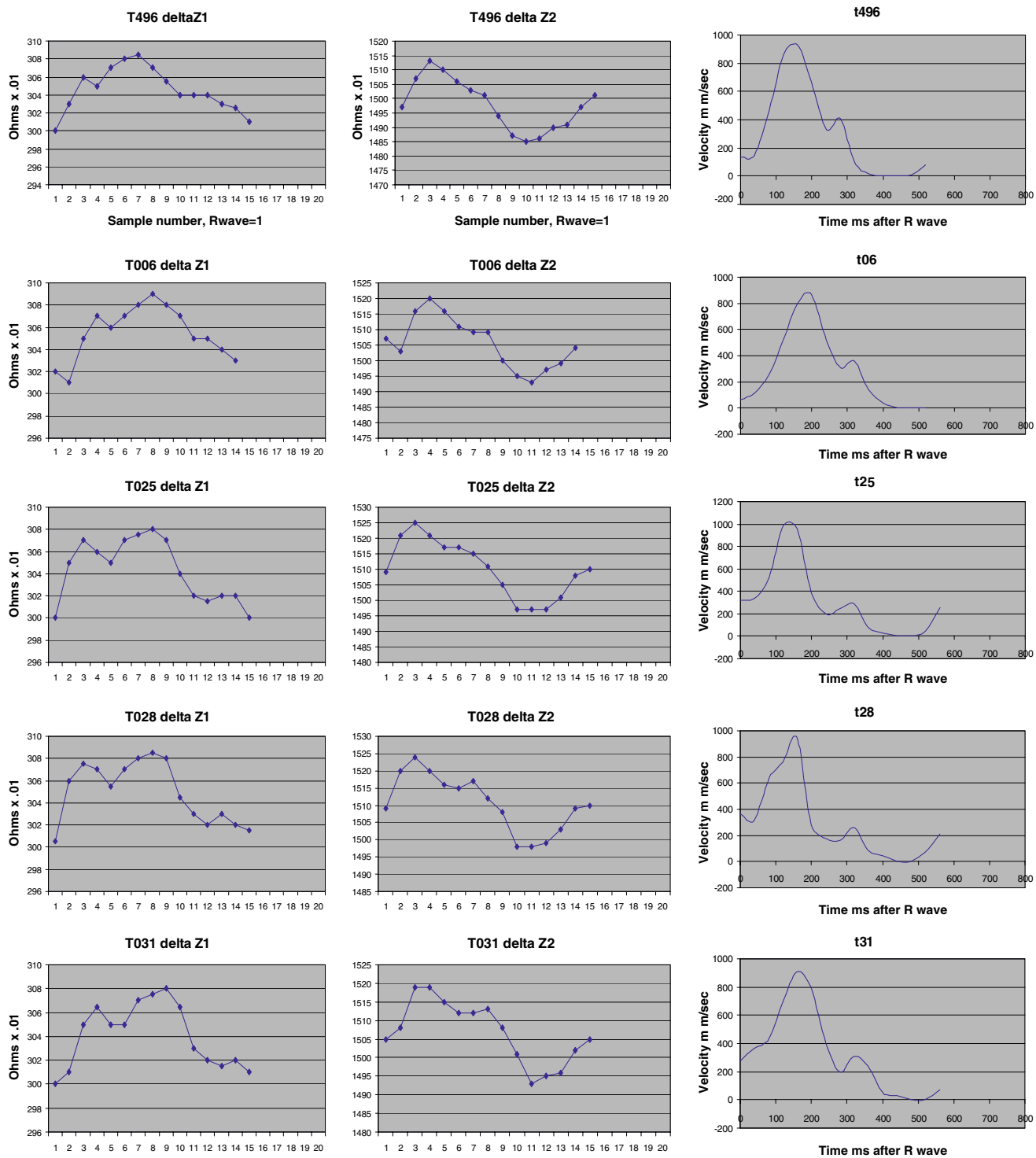

Fig. 3. Delta-Z traces and derived flow velocity for patient T. 40 ms per sample. Sample time starts with R wave of EKG = 1.

contribution to impedance change early in the impedance cycle, at least up to the maximum ΔZ change [43]. Aortic volume change ($\propto$R) is mathematically eliminated also. Thus the dual impedance method allows calculation of aortic blood flow velocity without requiring measurement of either **A** or **R**. Where **R** is necessary for the calculation

Table 2. Impedance data (×10 mΩ) for the three patients (S, K and T)

Record	R peak																			
S441 Z1	308	315	322	323	324	322	323	325	326	326	324.5	323	321	322.5	321	319	318	312	308	
S441 Z2	1380	1384	1388	1386	1381	1373	1366	1367	1368	1369	1371	1375	1376	1381	1385	1392	1395	1381	1375	
S448 Z1	305	309	315.5	319	318	318	317	319.5	320.5	322	319	318	317.5	318	316.5	316	312	306		
S448 Z2	1366	1372	1373	1377	1366	1361	1353	1354	1358	1360	1361	1367	1368	1370	1376	1381	1374	1364		
S453 Z1	304	308	312	312	312.5	314	315.5	316.5	317	316	315.5	314.5	315	315.5	312	312	311	305	303	
S453 Z2	1362	1362	1362	1357	1351	1345	1341	1342	1344	1346	1352	1356	1360	1363	1365	1378	1375	1361	1358	
S467 Z1	332.5	333.5	340	340.5	338	338	338	340	341	341.5	341	342	342	345	345.5	342.5	343	339	334	
S467 Z2	1366	1370	1372	1371	1358	1352	1346	1348	1350	1353	1356	1361	1365	1377	1381	1384	1391	1376	1361	
S470 Z1	332	336	340	340	337	336	336	340	340	340	339	340	341	345	343	340	341	336	331	331
S470 Z2	1365	1371	1369	1365	1355	1350	1344	1349	1350	1355	1357	1365	1372	1379	1382	1384	1392	1372	1362	1365
S474 Z1	335	336	342	343.5	340	339	338	340	342	342	341	342.5	345	347	346	345	342	336	334	
S474 Z2	1365	1371	1372	1372	1354	1349	1341	1343	1347	1351	1353	1365	1372	1383	1386	1395	1386	1362	1359	
T496 Z1	300	303	306	305	307	308	308.5	307	305.5	304	304	304	303	302.5	301					
T496 Z2 (+500)	1497	1507	1513	1510	1506	1503	1501	1494	1487	1485	1486	1490	1491	1497	1501					
T006 Z1	302	301	305	307	306	307	308	309	308	307	305	305	304	303						
T006 Z2	1507	1503	1516	1520	1516	1511	1509	1509	1500	1495	1493	1497	1499	1504						
T025 Z1	300	305	307	306	305	307	307.5	308	307	304	302	301.5	302	302	300					
T025 Z2	1509	1521	1525	1521	1517	1517	1515	1511	1505	1497	1497	1497	1501	1508	1510					
T028 Z1	300.5	306	307.5	307	305.5	307	308	308.5	308	304.5	303	302	303	302	301.5					
T028 Z2	1509	1520	1524	1520	1516	1515	1517	1512	1508	1498	1498	1499	1503	1509	1510					
T031 Z1	300	301	305	306.5	305	305	307	307.5	308	306.5	303	302	301.5	302	301					
T031 Z2	1505	1508	1519	1519	1515	1512	1512	1513	1508	1501	1493	1495	1496	1502	1505					
K054 Z1	314	309	307	304.5	302	303	302	303	303.5	302.5	303	303	303.5	303.5	307	312	313.5			
K054 Z2	1704	1697	1694	1689	1677	1672	1670	1672	1675	1673	1675	1676	1677	1678	1685	1701	1703			
K056 Z1	314.5	311	308.5	306.5	302	302	301.5	301.5	302.5	303	302	302.5	302.5	302.5	305	312	313			
K056 Z2	1702	1694	1690	1685	1672	1666	1663	1663	1664	1666	1666	1667	1668	1669	1673	1692	1698			
K076 Z1	348.5	345	339	339.5	338.5	341	344.5	346	347	348	350	353	355.5	357	356	355	354	353	352	350
K076 Z2	1624	1617	1605	1602	1600	1608	1619	1622	1624	1625	1626	1629	1632	1633	1631	1629	1628	1628	1629	1628
K079 Z1	345	341	335	335	335.5	339.5	343	344.5	345	346	348	352	354	354.5	352	350	348	346		
K079 Z2	1614	1607	1596	1590	1593	1603	1615	1619	1621	1621	1623	1627	1631	1632.5	1629	1628	1625	1619		
K083 Z1	346.5	344.5	338	335	332.5	333.5	337	338.5	340	343	345	348	352	353	352.5	352	351	350	349	348
K083 Z2	1616	1614	1598	1589	1590	1591	1600	1608	1611	1614	1615	1618	1624	1628	1627	1624	1622	1622	1623	1620

R peak of EKG synchronised to first column of impedance results.

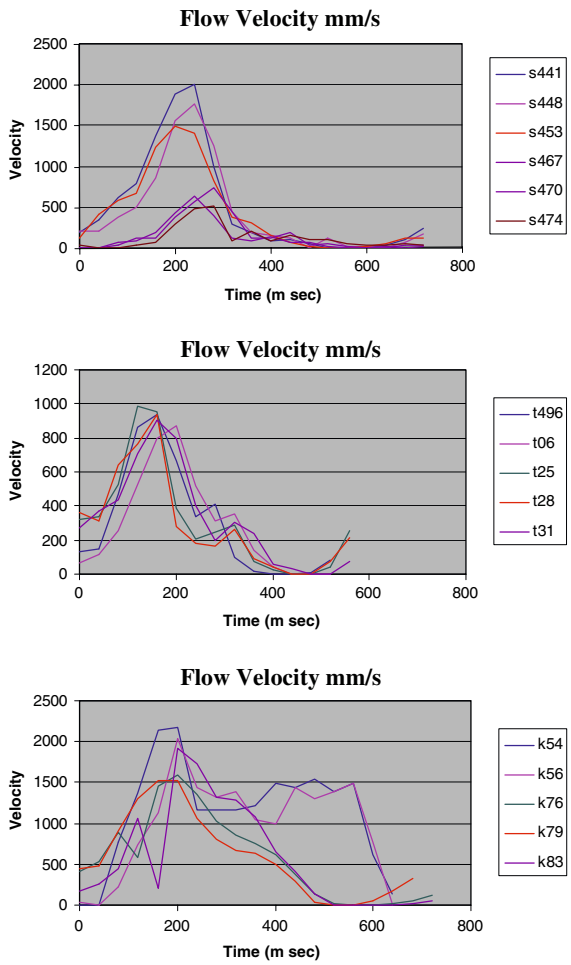

Fig. 4. Instantaneous aortic blood flow velocity data from three patients. Sample time starts with R wave of EKG.

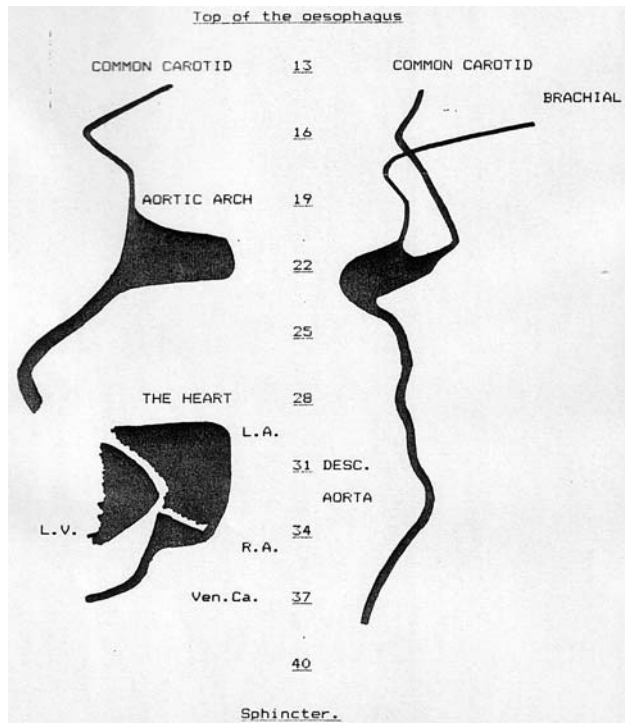

Fig. 5. Anatomy of the major blood vessels relative to the esophagus. A schematic representation showing the proximity, to the esophagus, of the major vessels and heart at different levels of the thorax measured from the teeth to demonstrate the likely confounding effects on esophageal impedance measurements from blood velocity movement in such structures. Derived from CT images by the authors.

of aortic stroke volume it may be estimated (~1.25 cm in adults) or measured by ultrasound, CT or MRI. Figure 2 shows typical ΔZ waveforms. The rapid negative impedance change at the start of systole is probably due only to the flow of blood in the aorta, not aortic movement. This view is also shared by Visser et al. [39, 40], but contradicts the result of Mitchell and Newbower [34] who claimed from their theoretical study that the major component of the intrathoracic impedance was not due to blood flow at all. Visser [39, 40] also describes the effect of hematocrit on the impedance change of flowing blood, and this is taken into account in Equation (2) and subsequently Equations (3) and (4). For absolute aortic velocity calculations the correct hematocrit should be used to generate the constants **a** and **b** in Equations (2)–(4) [40], but use of the "standard" values for an hematocrit of 45% will allow consistent velocities to be measured in any individual subject. Shear forces from both longitudinal and rotational flow in the aorta will align the red blood cells to generate the measured impedance changes, however the rotational component will contribute less than 10%, because the red blood cells align themselves with their large diameter along the major shear lines giving rise to the impedance change associated with flow and rotational flow will not change this orientation. This model depends on the change in impedance when blood flows as modelled by Visser [39, 40] who investigated hematocrits of 36.4%, 47.5% and 53.7% deriving his equation from these results, and which does not distinguish between forward or reverse blood flow. There may be other factors which influence the impedance change such as blood flow turbulence and acceleration effects (in both the aorta and the nearby heart and lungs), which may need to be considered in subsequent models if controlled experiments indicate a significant effect. Our good aortic velocity profiles suggest that these effects, if active, do not contribute greatly to the overall impedance changes.

The variations in the latter part of the impedance waveforms suggest that aortic movement or other effects, such as changes in the diameter of the aorta and

decelerating flow, are dominant in this part of the waveform after the peak impedance change. These variations are most probably complicated by the different anatomical relationships of the esophagus to the aorta and heart in that region, which have not been modelled yet. Anatomical variation between animals and man is particularly important to take into account when testing this dual electrode intrathoracic impedance method. Aortic displacement in a relatively more mobile mediastinum is likely in animals. Thus, although the maximum $|\Delta Z|$ excursion can be consistently measured, variations in the latter part of the wave prevent reliable estimation of blood flow or of aortic valve closure time (t_2) from this part of the impedance trace, unlike the transthoracic method where it is claimed [10] that a consistent ΔZ signal occurs to mark aortic closure. This valve closure time is more conveniently measured instead by using a microphone attachment on the esophageal probe to record heart sounds. Accurate information on timing of cardiac cycle events allows cardiac contractility indices such as systolic time intervals, dP/dt, dV/dt and the Heather Index (dZ/dt(max)/PEP Ωs^{-2}) [59] to be computed if required. When combined with other easily measured parameters from the esophageal probe, such as ECG and the phonocardiogram, even more information may be generated [35]. This variability after the maximum $|\Delta Z|$ can be ignored for calculation of stroke volume because there is minimal aortic movement until after peak flow [43]. This assumption is only needed for calculation of aortic stroke volume.

Recently Hettrick et al. [60] have again confirmed that the impedance signal is dependent on position of the electrodes. Unlike Mitchell and Newbower [34], when using internal esophageal electrodes only, they showed that the conductance was closely associated with normalized aortic diameter with no consideration of aortic displacement. They did not consider the relationship of their signal to aortic blood flow. Our model allows elimination of aortic diameter and aortic displacement with focus on aortic blood flow.

With the intrathoracic approach to estimation of aortic blood flow, there are obviously other impedance signals present, from the heart and other closely associated blood vessels, which contribute to the measured impedance change (Figure 5). These other factors may be either additive or subtractive depending on the direction of movement of organs, vessels or blood flow. The distance of the aorta from the esophageal probe is critical as the impedance signal rapidly falls off with distance as shown in Figure 6. This diagram shows that for all configurations of the voltage sensing electrodes there is a rapid fall off in the ΔZ signal when blood movement occurs more than 2 cm from the electrodes (i.e. when $\mathbf{A} > 2$ cm). It also demonstrates that the biggest signal is obtained when the

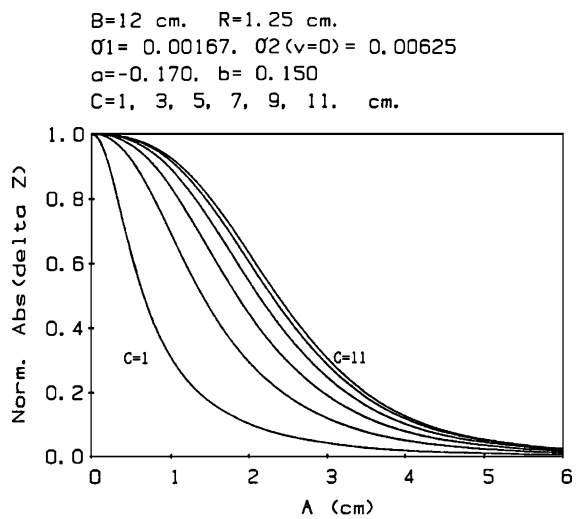

Fig. 6. Dependence of ΔZ on A (esophageal-aorta separation) for several values of C (measurement electrode spacing): Simulation results. The greatest signal occurs when the voltage sensing and current source electrodes are closest together (i.e. B–C < 4 cm). For the configurations of the voltage sensing electrodes (C1–C11) there is a rapid decline in ΔZ signal as the distance between the aorta and the esophagus increases.

voltage sensing and current source electrodes are closer together (i.e. when $\mathbf{B}$–$\mathbf{C} < 4$ cm). Because of the position of the descending aorta near the distal esophageal electrodes, the heart and a segment of the left lung are the only close organs within the critical 2 cm distance. There will only be a very small contribution to the impedance signal from changes in the lung blood volume and the random directional changes due to blood flow in the lung will cancel out. The heart will possibly have an effect on impedance changes depending on its size and position in relationship to the esophageal electrodes. However aortic blood flow changes will be the major contribution to impedance changes at this level of the descending aorta. Hopefully, with better understanding of the total intrathoracic impedance field, more precise positioning of the probe, and more subtle mathematical analysis, a more accurate comparison will be achieved. More elaborate studies on impedance fields such as that by Sakamoto and others [61–65] will help in this regard.

There may be other possible problems with the intrathoracic placement of the esophageal probe when there is a dilated left atrium, or cardiomegaly impinging on the esophagus, when there is an hiatus hernia, or where there is misplacement of the probe within the esophagus either from the start or movement with time. Possibly a better technique for positioning the esophageal probe would be to use the esophageal EKG as a marker to position the distal electrodes. Our experience with unsuccessful recordings in two patients suggests that the position of the

electrodes is crucial and may prove to be a troublesome issue with this technique, but nevertheless we have demonstrated that there is valuable aortic flow information easily available.

As well as the possible theoretical problems, which are not yet fully understood, there are also other specific problems that may be occurring in these post-cardiac surgery patients. In addition to the normal anatomical variation between patients, many of these particular patients will also have extensive aortic vascular disease which may be a crucial factor influencing the impedance measurement. Such aortic pathology could influence aortic blood flow, distance of the probe from the aorta, radius of the aorta, aortic translational movement, and also the relationship of peak flow to aortic translational movement, if any. As Raaijmakers and her colleagues have recently re-emphasised ''great care should be taken when transthoracic impedance cardiography is applied to cardiac patients'' [29]. Such factors are most likely to have caused the measurement problems in the patients whose results could not be computed, and contributed to the comparative differences in the cases where results were obtained. Early studies [66, 67] with the transthoracic impedance method, particularly with cardiac patients, were poor though refinements with non-cardiac patients have shown much better results [11, 26, 27]. Animal experiments using electromagnetic flow probes around the descending aorta would provide a better test of the mathematical models but were not available to us.

Using two pairs of voltage sensing electrodes in the esophagus simultaneously in this dual impedance method we have obtained flow profiles for blood flow in the descending aorta (Figure 4). This latter technique allows any adverse effects caused by changing **A** and/or **R** to be cancelled out mathematically without their values being known. The responsiveness of the method to blood flow conductivity changes is thereby increased. The shape of the impedance traces (Figures 2 and 3) [68, 69] is very different from that recorded by surface electrodes [5, 6]. Indeed, the shape is different from subject to subject which is probably due to small differences in position in the esophagus vis à vis the descending aorta. However, because simultaneous measurements are being used to remove the most significant unknown variable, the distance between the esophageal probe and the aorta, **A**, from the equations, a credible velocity trace is obtained [70].

Although, as we have shown descending aortic stroke volume may be calculated this does not materially assist in calculating cardiac output, because of the variable contribution of descending aortic blood flow to total cardiac output. Recently Wallace et al. [71] have introduced an endotracheal impedance device with three orthogonal pairs of electrodes attached to the cuff of an endotracheal tube, which is positioned ''close'' to the ascending aorta. A new equation based on Bernstein/Sramek [50] and on a modified Simpson's integral of the Patterson/Kubicek equation by Shmulewitz [72] has shown promise but still requires calibration particularly between individuals. Because of the position of their electrodes around the cuff of the endotracheal tube, and because the cuff is likely to be positioned in humans high in the cervical trachea just below the vocal cords which is some distance from the ascending aorta, the electrode signals are unlikely to be as specific to aortic flow as the authors suggest because of the effects of distance from the signal source (see Figure 5). If a more central thoracic position of the endotracheal tube could be assured then the electrodes would be positioned closer to the ascending aorta, and such a position would allow the use of our dual electrode method to calculate ascending aortic blood flow which would provide a better estimate of stroke volume than from the descending aorta.

Our model shows that some of the changes due to anatomical factors may be eliminated allowing measurement of aortic blood flow velocity. There will be other factors which will affect the results which still need to be defined before they are able to be excluded or included in more sophisticated mathematical models. We believe, however, that we have extended the model of Mitchell and Newbower [34] using both the aortic blood-flow effect on impedance and the dual-impedance method. These improvements allow aortic flow velocity to be calculated along with descending aortic stroke volume. We believe, by optimising the anatomical electrode position (both in the probe and within the esophagus), using more sophisticated theoretical models (such as more probe electrodes and combinations of intrathoracic and transthoracic electrodes, 3-D and tomographic models for better anatomical modelling) with more elaborate mathematical solutions, and using more precise methods of impedance measurement, that better estimates of aortic flow velocity and stroke volume are achievable.

CONCLUSION

A new theoretical intrathoracic impedance model and method has been developed using an esophageal electrical impedance probe to estimate the aortic blood flow velocity, and tested in a small number of patients. This method uses a dual set of impedance electrodes to eliminate the anatomical effects of aortic distension or displacement on intrathoracic impedance change during aortic blood flow. The impedance change with aortic blood flow is then dominant which allows an extension of the model described in 1979 by Mitchell and Newbower

[34] to measure directly aortic blood flow velocity, and to estimate the descending aortic component of left ventricular stroke volume. This intrathoracic electrical impedance method requires further analytical work in order to assess the contributions to the signal from the cardiovascular structures in the vicinity of the electrodes. However, we have shown that there is significant aortic flow information readily accessible within the intrathoracic impedance signal, and that this information has potential for aortic stroke volume measurement.

REFERENCES

1. Nyboer J, Bagno S, Barnett A, Halsy RH. Radiocardiograms – the electrical impedance changes of the heart in relation to electrocardiograms and heart sounds. J Clin Invest 1940; 19: 773.
2. Holzer W, Polzer K, Marko A. RKG, Rheokardiographie, ein Verfahren der Kreislaufforschung und Kreislaufdiagnostik. Verlag Wilhelm Maudrich, Wien 1945; pp. 46 (RKG Rheocardiography, a method of circulation's investigation and diagnosis in circular motion. Authorized English translation by EM Kreidl Wilhelm Maudrich, Vienna 1946; pp 43).
3. Nyboer J. Impedance plethysmography. In: Glasser, O ed., Medical Physics. 2Year Book Publishers, Chicago, 1950: 736–743.
4. Nyboer J. Electrical impedance plethysmography, Charles Thomas: Springfield, 1959, pp. 243.
5. Kubicek WG, Karnegis JN, Patterson RP, Witsoe DA, Mattson RH. Development and evaluation of an impedance cardiac output system. Aerospace Med 1966; 37: 1208–1212.
6. Kubicek WG, Patterson RP, Witsoe DA. Impedance cardiography as a non-invasive method of monitoring cardiac function and other parameters of the cardio-vascular system. Ann NY Acad Science 1970; 170: 724–732.
7. Lababidi Z, Ehmke DA, Durnin RE, Leavorton PE, Lauer RM. The first derivative thoracic impedance cardiogram. Circulation 1970; 41: 651–658.
8. Van de Water JM, Mount BE, Barela JR, Schuster R, Leacock FS. Monitoring the chest with impedance. Chest 1973; 64: 597–603.
9. Kubicek WG, Kottke FJ, Ramos MU, Patterson RP, Witsoe DA, Labree JW, Remole W, Layman TE, Schoening H, Garamela JT. The Minnesota impedance cardiograph – theory and applications. Biomed Eng 1974; 9: 410–416.
10. Mohapatra SN. Non-invasive cardiovascular monitoring by electrical impedance technique, Pitman Medical: London, 1981, pp. 282.
11. Lamberts R, Visser KR, Zijlstra WG. Impedance cardiography, Van Gorcum: Assen, 1984, pp. 160.
12. Kubicek WG. On the source of peak first time derivative (dZ/dt) during impedance cardiography. Ann Biomed Eng 1989; 17: 459–462.
13. Clarke DE, Raffin TA. Thoracic electrical bioimpedance measurement of cardiac output – not ready for prime time. Crit Care Med 1993; 21: 1111–1112.
14. van der Meer BJM, Woltjer HH, Sousman AM, Schreuder WO, Bulder ER, Huybregts MAJM, de Vries PMJM. Impedance cardiography – importance of the equation and the electrode configuration. Intens Care Med 1996; 22: 1120–1124.
15. MacGregor DA, Royster RL. Perfecting the imperfect. Crit Care Med 1999; 27: 2311–2312.
16. Sageman WS, Riffenburgh RH, Spiess BD. Equivalence of bioimpedance and thermodilution in measuring cardiac index after cardiac surgery. J Cardiothorac Vasc Anesth 2002; 16: 8–14.
17. Bernstein DP, Lemmens HJM. Stroke volume equation for impedance cardiography. Med Biol Eng Comput 2005; 43: 443–450.
18. Cremer M. Uber die Registrierung mechanischer Vorgange auf elektrischem Wege, speziell mit Hilfe des Saitengalvanometers und Saitenelektrometers. Munch Med Wschr 1907; 33: 1629–1630.
19. Atzler E, Lehmann G. Uber ein neues Verfahren zur Darstellung der Herztatigkeit (Dielektrographie). Arbeitsphysiologie 1932; 5: 636–680.
20. Rosa L. Diagnostische Anwendung des Kurzwellenfeldes in der Herz- und Kreislaufpathologie (Radiokardiographie). Z Kreislaufforsch 1940; 32: 118–135.
21. Schuster H, Schuster C, Gilfrich H, Scholmerich P. Transthoracic electrical impedance during extra-corporeal haemodialysis in acute respiratory failure (shocked lung syndrome). Intens Care Med 1980; 6: 147–154.
22. Roos J, Koomans HA, Boer P, Dornhout Mees EJ. Transthoracic electrical impedance as an index of extra-cellular fluid volume in man. Intens Care Med 1985; 11: 39–42.
23. Teo KK, Hetherington MD, Haernel RG. Cardiac output measured by impedance cardiography during maximal exercise tests. Cardiovasc Res 1986; 19: 737–743.
24. Fuller HD. The validity of cardiac output measurement by thoracic impedance: a meta-analysis. Clin Invest Med 1992; 15: 103–112.
25. Jensen L, Yakimets J, Teo KK. A review of impedance cardiography. Heart Lung 1995; 24: 183–193.
26. Shoemaker WC, Belzberg H, Wo CCJ, Milzman DP, Pasquale MD, Baga L, Fuss MA, Fulda GJ, Yarbrough K, Van DeWater JP, Ferraro PJ, Thangathurai D, Roffey P, Velmahos G, Murray JA, Asensio JA, ElTawil K, Dougherty WR, Sullivan MJ, Patil RS, Adibi J, James CB, Demetriades D. Multicenter study of noninvasive monitoring systems as alternatives to invasive monitoring of acutely ill emergency patients. Chest 1998; 114: 1643–1652.
27. Shoemaker WC, Thangathurai D, Wo CCJ, Kutcha K, Canas M, Sullivan MJ, Farlo J, Roffey P, Zellman V, Katz RL. Intraoperative evaluation of tissue perfusion in high-risk patients by invasive and noninvasive hemodynamic monitoring. Crit Care Med 1999; 27: 2147–2152.
28. Newman DG, Callister R. The noninvasive assessment of stroke volume and cardiac output by impedance cardiography: a review. Aviat Space Environ Med 1999; 70: 780–789.
29. Raaijmakers E, Faes TJC, Scholten RJPM, Goovaerts HG, Heethaar RM. A meta-analysis of three decades of validating thoracic impedance cardiography. Crit Care Med 1999; 27: 1203–1213.
30. Rosenberg P, Yancy CW. Noninvasive assessment of hemodynamics: an emphasis on bioimpedance cardiography. Curr Opin Cardiol 2000; 15: 151–155.
31. American Society of Anesthesiologists. Task force on pulmonary artery catheterization: practice guidelines for pulmonary artery catheterization. Anesthesia 1993; 78: 380–394.

32. Chernow B. Pulmonary artery floatation catheters: a statement by the American College of Chest Physicians and the American Thoracic Society. Chest 1997; 111: 261–266.
33. Guyatt G, Ontario Intensive Care Study Group. A randomized controlled trial of right heart catheterization in initial care of critically ill patients. J Intens Care Med 1991; 6: 91–95.
34. Mitchell MM, Newbower RS. Intra-thoracic electrical impedance measurements from an esophageal probe. Am J Physiol 1979; 236: R168–R174.
35. Baker AB, McLeod CN. Oesophageal multipurpose monitoring probe. Anaesthesia 1983; 38: 892–897.
36. Baker AB, Roxburgh AJ. Intra-thoracic impedance plethysmography and cardiac output. Proc Otago Med Sch 1984; 62: 12–14.
37. Balestra B, Malacrida R, Leonardi L, Suter P, Malone L. Esophageal electrodes allow precise assessment of cardiac output by bio-impedance. Crit Care Med 1992; 20: 62–67.
38. Coulter NA, Pappenheimer JR. Development of turbulence in flowing blood. Am J Physiol 1949; 159: 401–408.
39. Visser KR, Lamberts R, Korsten HHM, Zijlstra WG. Observations on blood flow related electrical impedance changes in rigid rubes. Pfluegers Arch 1976; 366: 289–291.
40. Visser KR. Electrical properties of flowing blood and impedance cardiography. Ann Biomed Eng 1989; 17: 463–473.
41. Baker AB, Roxburgh AJ, McLeod C. Intra-thoracic impedance and aortic blood flow. Proc Otago Med Sch 1984; 62: 69–70.
42. McDonald DA. Blood flow in arteries. 2nd edn. Edward Arnold: London, 1974, pp. 113–117.
43. McDonald DA. Blood flow in arteries. 2nd edn. London: Edward Arnold, 1974: 119, 286–288.
44. Kedrov AA, Liberman TV. On the so called rheocardiography [in Russian]. Klin Med (Mosk) 1949; 3: 40 (Exerpta Medica 1417).
45. Bonjer FH. Circulatieonderzoek door impedantiemeting. Thesis. Groningen, Netherlands, 1950.
46. Nyboer J. Electrical impedance plethysmography. A physical and physiologic approach to peripheral vascular study. Circulation 1950; 2: 811–821.
47. Patterson RP. Cardiac output determinations using impedance plethysmography. MSc thesis. University of Minnesota, USA, 1965.
48. Critchley LAH. Impedance cardiography. The impact of new technology. Anaesthesia 1998; 53: 677–684.
49. Sramek BB. Hemodynamic and pump-performance monitoring by electrical bioimpedance: new concepts. Problems in Resp Care 1989; 2: 274–290.
50. Bernstein DP. A new stroke volume equation for thoracic electrical bioimpedance: theory and rationale. Crit Care Med 1986; 14: 904–909.
51. De Mey C, Enterling D. Non-invasive assessment of cardiac performance by impedance cardiography: disagreement between two equations to estimate stroke volume. Aviat Space Environ Med 1988; 59: 57–62.
52. Sageman WS, Amundson DE. Thoracic electrical bioimpedance measurement of cardiac output in postaortocoronary bypass patients. Crit Care Med 1993; 21: 1139–1142.
53. Koobi T, Kaukinen S, Turjanmaa VMH. Cardiac output can be reliably measured noninvasively after coronary artery bypass grafting operation. Crit Care Med 1999; 27: 2206–2211.
54. Imhoff M, Lehner JH, Löhlein D. Noninvasive whole-body electrical bioimpedance cardiac output and invasive thermodilution cardiac output in high-risk surgical patients. Crit Care Med 2000; 28: 2812–2818.
55. Tishchenko MI. Estimation of the stroke volume by integral rheogram of the human body [in Russian]. Sechenov Physiol J 1973; 59: 1216–1224.
56. Patterson RP, Witsoe DA, From A. Impedance stroke volume compared with dye and electromagnetic flowmeter values during drug-induced inotropic and vascular changes in dogs. Ann NY Acad Sci 1999; 873: 143–148.
57. Smith DN. Bioimpedance measurement of cardiac output. Crit Care Med 1994; 22: 1513–1515.
58. Wang L, Patterson R. Multiple sources of the impedance cardiogram based on 3-D finite difference human thorax models. IEEE Trans Biomed Eng 1995; 42: 141–148.
59. Heather LW. A comparison of cardiac output values by the impedance cardiograph and dye dilution in cardiac patients. Progress Report Contract No. NAS9-4500 National Aeronautics and Space Administration, Houston 1969; 247–258.
60. Hettrick DA, Battocletti JH, Pagel PS, Vurek GG, Tessmer JP, Kersten JR, Warltier DC. Correlation of esophageal conductance measurements with aortic and left ventricular diameters and stroke volume. IEEE Trans Biomed Eng 2000; 47: 559–564.
61. Sakamoto K, Muto K, Kanai H, Iizuka M. Problems of impedance cardiography. Med Biol Eng Comput 1979; 17: 697–709.
62. Brown BH, Barber DC. Electrical impedance tomography; the construction and application to physiological measurement of electrical impedance images. Med Prog Technol 1987; 13: 69–75.
63. Eyuboglu BM, Brown BH, Barber DC. In vivo imaging of cardiac related impedance changes. IEEE Eng Med Biol 1989; 8: 39–45.
64. Dijkstra AM, Brown BH, Leathard AD. Clinical applications of electrical impedance tomography. J Med Eng Technol 1993; 17: 89–98.
65. Metherall P, Barber DC, Smallwood RH, Brown BH. Three-dimensional electrical impedance tomography. Nature 1996; 380: 509–512.
66. Bache RJ, Harley A, Greenfield JC. Evaluation of thoracic impedance plethysmography as an indicator of stroke volume in man. Am J Med Sci 1969; 258: 100–113.
67. Lababidi Z, Ehmke DA, Durnin RE, Leaverton PE, Lauer RM. Evaluation of impedance cardiac output in children. Pediatrics 1971; 47: 870–879.
68. Roxburgh AJ, Baker AB, Bannister P, McLeod C. Aortic blood flow from intra-thoracic impedance. Proc Otago Med Sch 1985; 63: 73–74.
69. McLeod CN, Baker AB, Roxburgh AJ, Bannister P. The aortic flow contribution to intrathoracic impedance – a simplified model and results. In: Proceedings IXth International Conference on Electrical Bio-Impedance. ICPRBI Uni. Heidelberg, Heidelberg. 1995: 145–147.
70. Nichols WW, O'Rourke MF. McDonald's blood flow in arteries 3rd edn. Edward Arnold: London, 1990, pp. 220.
71. Wallace AW, Salahieh A, Lawrence A, Spector K, Owens C, Alonso D. Endotracheal cardiac output monitor. Anesthesiology 2000; 92: 178–189.
72. Shmulewitz A. Apparatus and method of bioelectrical impedance analysis of blood flow. United States Patent 1998; 5: 782,774.